

www.acsami.org Research Article

Biotrapping Ureolytic Bacteria on Sand to Improve the Efficiency of Biocementation

Gizem Elif Ugur, Kylee Rux, John Connor Boone, Rachel Seaman, Recep Avci, Robin Gerlach, Adrienne Phillips, and Chelsea Heveran*



Cite This: ACS Appl. Mater. Interfaces 2024, 16, 2075–2085



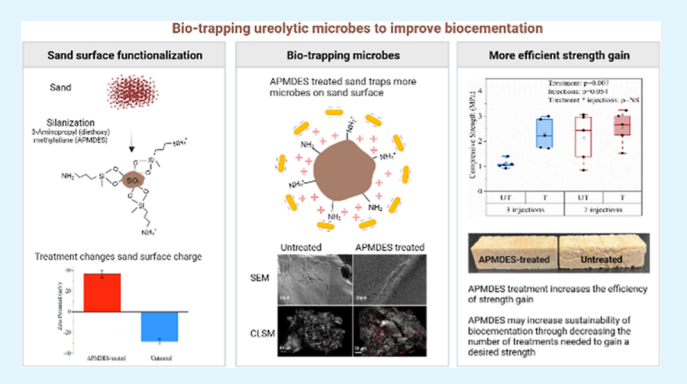
ACCESS I

III Metrics & More

Article Recommendations

s Supporting Information

ABSTRACT: Microbially induced calcium carbonate precipitation (MICP) has emerged as a novel technology with the potential to produce building materials through lower-temperature processes. The formation of calcium carbonate bridges in MICP allows the biocementation of aggregate particles to produce biobricks. Current approaches require several pulses of microbes and mineralization media to increase the quantity of calcium carbonate minerals and improve the strength of the material, thus leading to a reduction in sustainability. One potential technique to improve the efficiency of strength development involves trapping the bacteria on the aggregate surfaces using silane coupling agents such as positively charged 3-aminopropyl-methyl-diethoxysilane (APMDES). This treatment traps bacteria on sand through



electrostatic interactions that attract negatively charged walls of bacteria to positively charged amine groups. The APMDES treatment promoted an abundant and immediate association of bacteria with sand, increasing the spatial density of ureolytic microbes on sand and promoting efficient initial calcium carbonate precipitation. Though microbial viability was compromised by treatment, urea hydrolysis was minimally affected. Strength was gained much more rapidly for the APMDES-treated sand than for the untreated sand. Three injections of bacteria and biomineralization media using APMDES-treated sand led to the same strength gain as seven injections using untreated sand. The higher strength with APMDES treatment was not explained by increased calcium carbonate accrual in the structure and may be influenced by additional factors such as differences in the microstructure of calcium carbonate bridges between sand particles. Overall, incorporating pretreatment methods, such as amine silane coupling agents, opens a new avenue in biomineralization research by producing materials with an improved efficiency and sustainability.

KEYWORDS: biocementation, Sporosarcina pasteurii, microbial induced calcium carbonate precipitation (MICP), biotrapping, aminosilane functionalization

1. INTRODUCTION

The demand for infrastructure materials is continuously increasing. The impact of this high demand for concrete is that cement, the binding component of concrete, is the second most consumed resource in the world after water. The production of ordinary portland cement is responsible for generating 5-8% of global anthropogenic greenhouse gas emissions.² Alternative methods for manufacturing construction materials with greater sustainability are needed. Microbially induced calcium carbonate precipitation (MICP) has been the subject of considerable research interest for its potential to strengthen soils, seal cracks, and generate building materials through lower-temperature processes.^{3–8} The enzyme urease produced by ureolytic bacteria, such as Sporosarcina pasteurii (S. pasteurii), catalyzes urea hydrolysis to produce ammonium (NH_4^+) and carbonate ions (CO_3^{2-}) . In the presence of Ca^{2+} , the reaction becomes favorable for CaCO₃ precipitation (eqs 1 and 2).

$$CO(NH2)2 + 2H2O \xrightarrow{\text{urease}} 2NH4^+ + CO3^{2-}$$
 (1)

$$Ca^{2+} + CO_3^{2-} \rightarrow CaCO_3$$
 (2)

Strength development through MICP relies on establishing calcium carbonate bridges between aggregate particles, which serve to biocement the material. 6,8-10 It is well established that strength can be increased by increasing the quantity of calcium carbonate within the material, which is achieved through repeated injections of microbes and biocementation medium or higher concentrations of reactants. 9-12 Therefore, strength gain

Received: September 18, 2023 Revised: December 13, 2023 Accepted: December 21, 2023 Published: January 4, 2024





is usually achieved at the expense of sustainability. ^{3,13,14} Since the MICP reaction occurs in the immediate proximity of the bacteria, controlling the location of the bacteria could provide a new approach for improving the efficiency of strength development.

Attempts to control the bacterial spatial distribution for biocementation have been limited. One strategy was to adjust the salinity of the bacterial suspension or inject soil with saline solution to improve the retention of bacteria. However, this has important disadvantages, such as exposing bacteria to osmotic shock, thus potentially compromising microbial viability or activity, or increasing the risk of corrosion. 15 Another potential method to improve spatial control over MICP is to trap the bacteria on the aggregate surfaces using silane coupling agents. An example of this technology is BiyoTrap, 16 which functionalizes surfaces with 3-aminopropyl-methyl-diethoxysilane (APMDES). The chemical modification covalently attaches positively charged amine groups onto surfaces, which have hydroxyl groups, thus electrostatically attracting negatively charged walls of bacteria. ^{16–19} Silica sand already has hydroxyl moieties on its surface, 20 but the spatial density of these groups can be increased through ozone treatment. After APMDES treatment, bacteria are localized to the charged area but are not strictly immobilized. 16 APMDES and similar treatments have been utilized to rapidly detect trace amounts of bacteria in liquids such as drinking water sources and contaminated liquids, as well as to isolate sulfate-reducing bacteria. 16,21,22 Various surfaces have been successfully functionalized to biotrap bacteria, including silicon, glass, and glass wool fibers. 16, However, APMDES treatment has not yet been explored as a method to functionalize aggregates for the purpose of spatially controlling bacteria to achieve biocementation. The purpose of this study was to test the hypothesis that trapping bacteria on sand surfaces treated with APMDES would increase the efficiency of strength development during biocementation.

2. MATERIALS AND METHODS

2.1. Materials. *2.1.1. Sand.* Quikrete Commercial Medium Sand (#196251) was used in all the experiments. Sand was soaked in a 4% HCl solution overnight to remove the metal contaminants. Afterward, the pH was balanced to 7 by adding sodium bicarbonate before the sand was rinsed with tap water and left to air-dry at room temperature. After drying, the sand was sterilized by being autoclaved at 121 °C for 1 h.

2.1.2. Growth and Biocementation Media. The growth medium used for the starter culture contained 37 g L⁻¹ brain heart infusion (BHI) (Becton Dickinson, Franklin Lakes, NJ) and 20 g L⁻¹ urea (Fisher Scientific, Inc., Pittsburgh, PA) in deionized water. The biocementation medium (calcium-containing medium, CMM+) contained 3 g L⁻¹ Difco nutrient broth (BD, Franklin Lakes, NJ), 10 g L⁻¹ ammonium chloride (Fisher Scientific, Pittsburgh, PA), 20 g L⁻¹ urea (Fisher Scientific, Pittsburgh, PA), and 48 g L⁻¹ calcium chloride dihydrate (Fisher Scientific, Pittsburgh, PA) in deionized water. The growth medium (calcium-free medium, CMM-) used for the urea batch study contained 3 g L⁻¹ Difco nutrient broth (BD, Franklin Lakes, NJ), 10 g L⁻¹ ammonium chloride (Fisher Scientific, Pittsburgh, PA), and 20 g L⁻¹ urea (Fisher Scientific, Pittsburgh, PA) in deionized water and was adjusted to pH 6.3. All solutions were filter-sterilized using SteriTop 0.2 μm bottle top filters.

2.1.3. Molds for Generating Biocemented Structures. Interlocking molds for biocementation were designed with OnShape software and printed with a Prusa 3D printer using a polylactic acid (PLA) filament. Molds were designed with vertical slits of 0.4 mm width to facilitate the transport of bacterial suspensions and cementation medium (Figure S1). The inside dimensions of the molds were $50 \times 50 \times 50$ mm³. Prism-shaped molds with dimensions of 90 mm \times 25 mm \times 25 mm³ were also designed with a vertical slit of 0.4 mm.

2.2. APMDES Treatment of Sand. APMDES (Gelest Inc., Morrisville, PA) was used to functionalize the sand surface. APMDES forms a monolayer of aminosilanes and thus confers positive charges to the treated surface. ²⁵ This monolayer would be expected to maximize the number of active locations for electrostatic interactions with negatively charged cells. After the initial acid wash and autoclaving, the sand was sonicated in acetone for 15 min and then in ethanol for another 15 min to remove carbon contaminants from the surface. The sand was dried at 100 °C on a hot plate, placed in a UV Ozone chamber (BioForce NanoSciences, Ames, Iowa) for 15 min to increase hydroxyl (–OH) moieties and active sites for APMDES attachment, and subsequently immersed in a solution of 1% v/v APMDES in ethanol for 24 h. Sand was removed from the APMDES solution, rinsed in ethanol for 25 min to remove excess APMDES, and baked in an oven at 120 °C to remove polymerized APMDES from the surface.

X-ray photoelectron spectroscopy (XPS, Physical Electronics 5600) was used to verify the surface chemistry of the APMDES-treated sand. XPS was conducted under ultrahigh-vacuum conditions (\sim 8 × 10⁻¹⁰ Torr) using a monochromatic Al K α X-ray source (1486.6 eV photons) by monitoring the N 1s line and the chemical shifts associated with $-{\rm NH_2}$ and $-{\rm NH_3}^+$ species. Zeta potential measurements (Zeta-Meter System 4.0, Staunton, VA 24402) were used to confirm the surface charge of the sand after functionalization. Zeta potential was measured in neutral pH, deionized water, and data were collected for 50 sand grains per condition (untreated, APMDES-treated). XPS analyses were conducted to evaluate the quality and consistency of the APMDES treatment of the initial batches as a proof of concept. The zeta potential was used again to confirm the functionalization of subsequent batches.

2.3. Determining the Effect of APMDES Treatment on Microbial Growth, Viability, and Urea Hydrolysis. A 1 mL cryovial of thawed frozen S. pasteurii base stock (ATCC 11859) was added to 100 mL of BHI with 2% urea in an autoclaved 250 mL Erlenmeyer flask and incubated for 24 h on the orbital shaker at 150 rpm at 30 °C. One mL of starter culture was transferred into 100 mL of fresh BHI with 2% urea medium and incubated overnight (16 h). After the growth, approximately 40 mL of overnight culture was added to two 50 mL centrifuge tubes centrifuged at 6000 rpm for 10 min at 4 °C. The supernatant of both tubes was decanted and resuspended in CMM-. The optical density measured at 600 nm (OD₆₀₀) was adjusted to 0.4 by diluting in sterile CMM-. 200 μ L aliquots were transferred to a 96-well plate, and OD_{600} was measured using a Synergy HT reader (Biotek Instruments, Inc., Winooski, VT). The average OD_{600} of sterile media (CMM-) was subtracted from the OD₆₀₀ of bacterial culture to measure the OD_{600} of the culture without influence from the media or the 96-well plates.

To evaluate the effects of APMDES treatment on urea hydrolysis, microbial growth, and pH, 10 g of sand, APMDES-treated (n = 3) and untreated (n = 3), was mixed with 100 mL of CMM- and inoculated with 2 mL of the prepared bacterial cell suspension before being incubated at 30 °C on the orbital shaker at 150 rpm. Abiotic controls were prepared with 10 g of APMDES-treated sand (n = 1) and untreated sand (n = 1) in CMM-. To make APMDES-exposed media, 10 g of APMDES-treated sand was premixed with 100 mL of CMMmedia in a 250 mL Erlenmeyer flask and incubated overnight on the orbital shaker at 30 °C at 150 rpm, then filter-sterilized using SteriTop 0.2 μ m bottle top filters, and inoculated with 2 mL of bacterial suspension to evaluate the toxicity of treatment on microbial growth. Aliquots (1.5 mL) were collected in microcentrifuge tubes at each time point of 0, 1, 2, 4, 8, 12, 24, and 48 h to measure urea concentrations, OD, and pH. 60 μ L aliquots from microcentrifuge tubes were diluted in 540 µL of 1.2 M sulfuric acid (Fisher Scientific, Inc., Pittsburgh, PA) for a final dilution of 1:10 to use in a modified Jung assay to determine the urea concentration.2

Microbial viability after exposure to APMDES was evaluated by plating cultures. An overnight *S. pasteurii* culture was centrifuged at a setting of 2210 rpm for 10 min at 4 °C. The supernatant was removed and resuspended in phosphate-buffered saline solution (PBS) to provide bacteria with a stable environment and prevent interference by potential growth in fresh growth media. The OD was adjusted to 0.06 by adding fresh PBS to the residual pellet. A control that contained no

sand was also prepared. 1 mL of the S. pasteurii inoculum (OD 0.06) was added to 9 mL of PBS and diluted up to 10^8 -fold. Five 10 μ L samples from each dilution were plated on BHI agar plates and incubated at 30 °C for 24 h before colony-forming units (cfu) were counted for dilutions resulting in 3 to 30 colonies. 27 1.85 g of sand, APMDES-treated (n = 3) and untreated (n = 3), was added to 15 mL centrifuge tubes and inoculated with 3 mL of S. pasteurii culture in PBS $(OD_{600} = 0.06)$. The treatments were incubated for 1 h on the benchtop before 1 mL of the supernatant was sampled from all treatments, and serial dilutions and plating were performed. Following this step, for all centrifuge tubes containing sand, the microbial suspension was removed, sand was rinsed with 1 mL of PBS to remove loosely attached microbes, and 3 mL of PBS was added back into the tubes. All centrifuge tubes underwent a vortex-sonicate-vortex step (30 s for each) to detach microbes from sand. Serial dilutions and plating were once again conducted after detachment for groups containing S. pasteurii. Plates were incubated upside down in a 30 °C incubator for 24 h, and colony-forming units were recorded.

The influence of APMDES treatment on bacterial cell membrane integrity was evaluated through live/dead staining and confocal laser scanning microscopy imaging. After immersion in bacterial suspension $(OD_{600} = 0.6)$, sand samples were removed at 0 and 1 h to investigate the effects of the APMDES treatment on cell membrane integrity. Samples were stained with 200 μ L of a diluted 1:1 mixture of SYTO9 (live/green) and propidium iodide (red/membrane compromised) (LIVE/DEAD BacLight bacterial viability kit stain) (Invitrogen, catalog #L7012). Samples were rinsed three times with 200 μ L of Milli-Q water to remove excess dye and stored in the dark until imaging. Images were acquired with an upright Leica SP5 confocal laser scanning microscope using a 25× water immersion objective. The argon laser at 488 nm was used to excite off the fluorescent signal from viable cells (green color), and the signal was detected using photomultiplier tube detection (PMT) between wavelengths of 495 and 550 nm. The fluorescent signal from membrane-compromised cells (red color) was captured by excitation at 561 nm and emission between 595 and 650 nm. A laser beam scanned an area of interest at a frequency of 600 Hz.

2.4. Determining the Effect of APMDES Treatment on Microbial Attachment to Sand Grains. Scanning electron microscopy (SEM, Zeiss Supra 55VP) was used to investigate the surface microstructure and morphology of sand grains after immersion in bacterial suspensions and exposure to biocementation media. Elemental composition was obtained using an AZtec EDX (Oxford Instruments) detector. To investigate the microbial attachment on sand grains, 0.6 g of sand was inoculated with each 1 mL bacterial suspension (OD $_{600} = 0.6$) in microcentrifuge tubes, then the bacterial suspension was removed at 0.25, 1, and 16 h using a pipet, and samples were left to air-dry at room temperature. Air-dried samples were mounted on SEM stubs using conductive carbon tabs (PELCO, Ted Pella, Inc., Ca) and sputter coated with gold (Ted Pella 108 Carbon Coater) for 45 s to increase conductivity for high-resolution imaging.

2.5. Preparation of Biocemented Cubes. A starter culture was prepared by thawing 1 mL of frozen *S. pasteurii* base stock (ATCC 11859) and adding it to 100 mL of autoclaved BHI in a 250 mL Erlenmeyer flask. The flask was incubated for 24 h on an orbital shaker at 150 rpm and 30 °C. A fresh bacterial culture was then made by diluting the starter culture to 1:100 in sterile BHI and incubating it for an additional 24 h on the orbital shaker table at 150 rpm. The culture volume was approximately 50% of the flask volume to provide oxygen for the optimized bacterial growth. After 24 h, the OD₆₀₀ was measured from 200 μ L aliquots in flat-bottom 96-well plates using a Synergy HT reader (Biotek Instruments, Inc., Winooski, VT). The average OD₆₀₀ of sterile BHI was subtracted from the OD₆₀₀ of the bacterial culture, and the OD₆₀₀ of the culture was adjusted to 0.6 by diluting in sterile BHI.

Biocemented cubes were manufactured using APMDES-treated and untreated sand. First, 3D-printed cube molds were filled with 185 g of sand. Replicates (n = 5) were prepared for each condition. Each mold was immersed in 300 mL of bacterial suspension ($OD_{600} = 0.6$) for 16 h and then in biocementation medium for 8 h. Biocementation was carried out by repeating the above immersion procedure (16 h in bacterial suspension and 8 h in biocementation media) for 3 and 7 days

at room temperature using freshly made bacterial suspensions and biocementation media. To measure urea concentration using the Jung assay protocol, 60 μ L aliquots were collected from biocementation medium at 0, 1, 2, 4, and 8 h and diluted into 540 μ L of 1.2 M sulfuric acid (Fisher) for a final dilution of 1:10. Specimens were demolded, rinsed under tap water, and left to dry at 60 °C for a week. The weight of the cubes was recorded over time until equilibrium was reached. Additional specimens were manufactured as 25 × 25 × 90 mm³ prisms (Figure 9C).

2.6. Determination of Compressive Strength. Biocemented cubes were subjected to unconfined compression testing in accordance with ASTM D2166/D2166M. The specimens were subjected to compression until failure using a constant load rate of $0.013 \, \text{kN/s}$ on an MTS Criterion model 64. All replicates (n = 5) for each condition were tested, and the height and area of each cube were recorded prior to testing.

2.7. Evaluation of Biomineral Content and Mineralogical Characteristics. After compressive strength testing, biocemented cubes were acid digested to estimate the calcium carbonate content. Samples were collected from the edge (n=4) and middle (n=3) regions per cube. Two grams of sample were placed in a 15 mL centrifuge tube, and 10 mL of 10% nitric acid were added to each tube and incubated at room temperature for 24 h to digest calcium carbonate. Calcium concentrations were measured in the supernatant, the remaining supernatant was removed, and the samples were allowed to dry at 60 °C for 72 h prior to assessing the final mass. The obtained dry mass was used to calculate the weight percent of precipitated CaCO₃.

Subsamples of the biocemented cubes were ground to a fine powder using a pestle and mortar for XRD analyses. Crystalline phases of precipitated calcium carbonate on sand particles were examined using a Bruker D8 Advance powder X-ray diffractometer with a Cu K α source (λ = 1.54060 Å) at 40 kV and 40 mA; samples were scanned at angles from 5 to 75°, with a step size of 0.02°. The NIST Inorganic Crystal Structure Database (ICSD) was used to identify the crystal structure data.

Small pieces of cubes biocemented for 7 days were embedded in epoxy (Ted Pella Inc.) to compare the size distribution of the biocemented bridges on untreated and APMDES-treated sand. Embedded biocemented chunks were sectioned using a low-speed diamond saw (Isomet, Buehler, Lake Bluff, IL) and polished with 600 and 1200 grit wet silicon carbide paper (Buehler, Lake Bluff, IL) and then with Rayon fine cloths and different grades of alumina pastes (9, 5, 3, and 1 μ m). Sections were sonicated in tap water between polishing steps to remove impurities from the surface. Embedded sections were mounted on SEM stubs and carbon-coated (108C Auto SE Carbon Coater, Ted Pella Inc.) to avoid charging artifacts for SEM-EDS analysis. Elemental maps were generated for calcium and silicon at three randomly selected locations, each for three replicates of 7 day treated and untreated cubes (Zeiss SupraS5VP, working distance = 8.5, accelerating voltage = 10 kV, magnification 200×).

SEM-EDX elemental maps were processed with a custom MATLAB code to identify and measure sand grains (i.e., silicon-rich areas) and biomineral bridges (i.e., calcium-rich areas) (Figure S2). Images were binarized, thresholded using Otsu's method, ²⁸ subjected to dilation and erosion steps, and filtered to remove objects with areas less than 20 pixels. Measures included biomineral bridge areal number density, the ratio of biomineral bridge area to sand grain area, mean biomineral bridge area, major axis and minor axis lengths, and circularity (minor/major axis lengths).

2.8. Statistical Analysis. CaCO₃ content and compressive strength outcomes were compared between APMDES-treated sand and untreated sand using ANOVA. A three-factor mixed model ANOVA tested whether the weight percent of precipitated CaCO₃ depends on APMDES treatment, region, injections, and the interaction of these factors. A two-factor ANOVA tested whether compressive strength depends on APMDES treatment, the number of injections, or their interaction. To test the impact of calcium content on compressive strength, a linear mixed model was used with random effects of treatment and injections and a covariate of calcium content (analysis of

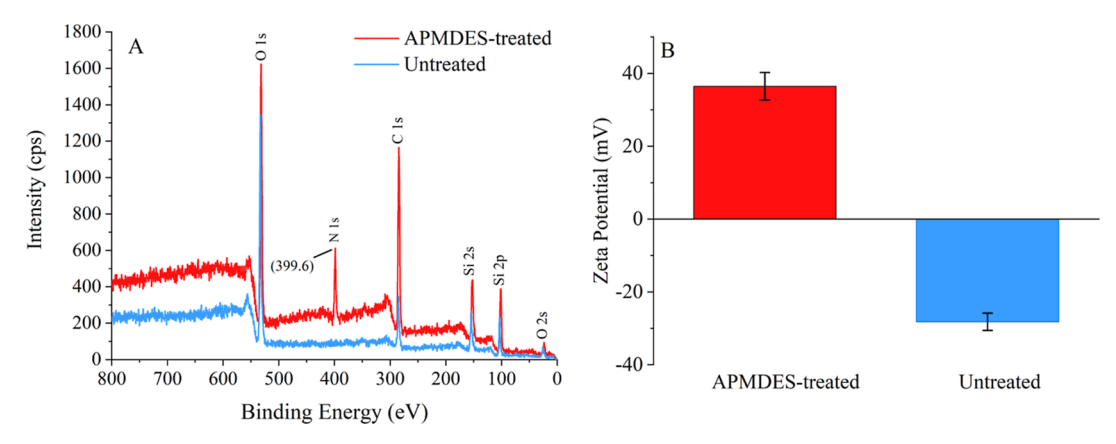


Figure 1. Change in the surface properties of sand with APMDES treatment. (A) XPS of sand grains before and after APMDES treatment confirmed the presence of amine groups with the peak at a binding energy of 399.6 eV (N 1s). (B) Zeta potential measurements of sand grains in distilled water, a neutral pH of 7, before and after APMDES treatment, n = 50 sand grains per group. Error bars represent 1 standard deviation.

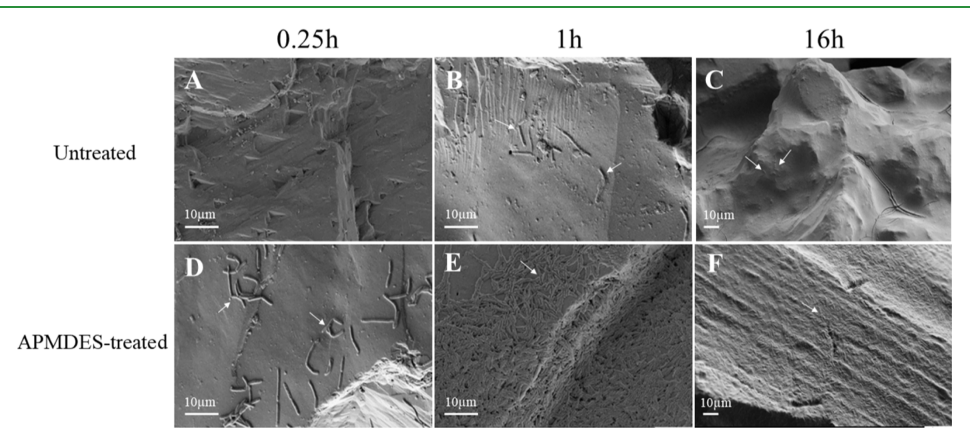


Figure 2. Initial attachment of *S. pasteurii* on APMDES-treated and untreated sand. (A–C) SEM indicates sparse attachment of microbes on untreated sand at 0.25 and 1 h and almost no attachment after 16 h of immersion. (D–F) APMDES-treated sand shows abundant attachment of microbes to the sand surface at 0.25, 1, and 16 h of immersion. At 1 h and 16 h, the microbes are seen as a dense mat. Scale bars are 10 μ m. White arrows indicate *S. pasteurii*.

covariance, ANCOVA). The influence of treatment on biomineral bridge characteristics was tested using a mixed-model ANOVA with the sample location as a random factor. All models were checked for residual normality and equal variance. If necessary, dependent variables were transformed to satisfy these assumptions. The statistical significance was defined a priori as p < 0.05. In the case of significant interactions in ANOVA models, posthoc tests were performed using a Fisher's least significant difference (LSD) test with family-wise error controlled using the Bonferroni procedure (i.e., critical alpha adjusted to 0.05/number of comparisons (2) = 0.025). Minitab (version 19.2020.1) was used for statistical analyses.

3. RESULTS AND DISCUSSION

3.1. APMDES Treatment Changes the Surface Properties of Aggregates and Localizes Bacteria on These Surfaces. Silane coupling agents, including APMDES and other closely related treatments, have been used to achieve biotrapping on a variety of surfaces, such as silicon and glass wool fibers, for nonbiocementation applications. This method of "biotrapping" bacteria does not cause strict immobilization unless coupled with antibodies but instead localizes (biotraps) bacteria within regions of treated surfaces, allowing bacteria to move freely near the surface of the sand particles. ¹⁶

XPS analysis was performed to confirm the elemental composition of the aggregates before and after APMDES

treatment. The XPS survey spectra of untreated sand showed the presence of Si (2p and 2s), O (1s), and C (1s) signals; the spectra of the APMDES-treated sand additionally revealed peaks at 399.6 eV corresponding to N (1s) amine groups, confirming the presence of amine moieties on the APMDES-treated sand (Figure 1A).

The amine groups (in particular, quaternary amine moieties) imparted a positive charge on the sand surfaces. A change in the zeta potential also indicated successful functionalization. The zeta potential of untreated sand was -28.18 mV and that of APMDES-treated sand was +36.47 mV (Figure 1B). Since the zeta potential of *S. pasteurii* is -67 mV, 30 electrostatic interactions between the positively charged APMDES-treated sand surface and the negatively charged wall of *S. pasteurii* likely promote bacterial trapping.

Imaging data confirmed the immediate localization of *S. pasteurii* on APMDES-treated sand surfaces, which under SEM appeared as a thin layer of cells (Figure 2). The bacterial attachment at 0.25, 1, and 16 h after immersion in bacterial suspension was greater on the APMDES-treated sand than that on the untreated sand. This length of time study was chosen because it represents the length of a biocementation treatment in this study (16 h). SEM micrographs showed few cells attached to untreated sand at 0.25, 1, and 16 h of immersion (Figure 2A—C). By contrast, APMDES-treated sand showed nearly

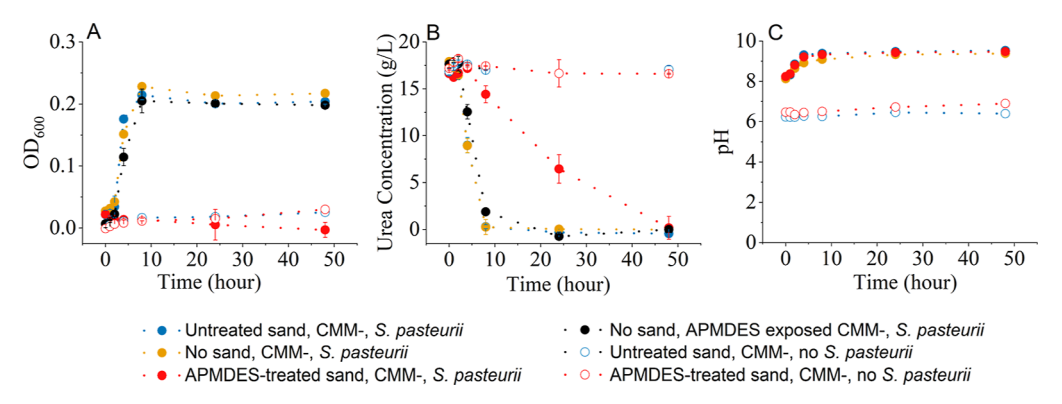


Figure 3. *S. pasteurii* growth, urea hydrolysis, and pH in batch reactors over 48 h. (A) OD increased over time for positive controls but not for APMDES-treated sand, indicating inhibition of growth; (B) urea concentration decreases rapidly for positive controls and also decreases, although less rapidly, for APMDES-treated sand; and (C) pH increased for all microbial cultures, regardless of APMDES treatment, which is expected during urea hydrolysis.

instantaneous bacterial adhesion at 15 min, abundant bacterial adhesion after 1 h of immersion, and a dense layer of microbes at 16 h (Figure 2D–F).

Together, these data confirm that APMDES treatment was successful in biotrapping bacteria on sand surfaces for time periods relevant to bacterial biocementation. This work is the first demonstration of the effective use of APMDES on sand surfaces. Sand is a common substrate for MICP-based biocementation that has many applications, such as manufacturing building materials and strengthening soils. Employing APMDES in the biocementation process would be expected to be useful for many of these applications, where the efficiency of biomineralization and/or strength development is appreciated. Whether APMDES would work as successfully on other types of aggregates was not investigated here but would be a valuable investigation.

3.2. APMDES Treatment Inhibits Bacterial Viability and Growth but Does Not Impede Urea Hydrolysis during Biocementation. A batch study was conducted to determine the influence of APMDES treatment on S. pasteurii growth and the hydrolysis of urea. The OD_{600} of the initial S. pasteurii inoculum was measured as 0.027. The growth curve of S. pasteurii in the presence of untreated sand was similar to the planktonic condition without sand, reaching an ${\rm OD}_{600}$ of 0.2 at 8 h. Bacterial growth was inhibited by the presence of APMDEStreated sand (Figure 3A), most likely due to the presence of -NH₃⁺ moieties, which are expected to be toxic. ^{17,31} Growth was slightly inhibited by APMDES in solution. However, even in the presence of APMDES-treated sand, urea hydrolysis and the resulting increase in pH in solution still occurred, albeit at slower rates (Figure 3B,C). Twenty g/L urea was almost completely hydrolyzed in 8 h for conditions without APMDES, while APMDES-treated sand required 48 h to hydrolyze most of the urea. The urea hydrolysis was likely slower in the presence of APMDES-treated sand because there was no bacterial growth that could increase the availability of the urease enzyme. This suggests that, despite inhibiting bacterial growth, APMDES does not interfere substantially with the activity of the S. pasteurii

After establishing that APMDES impeded *S. pasteurii* growth, we assessed the impact of the treatment on viability. Viability was determined from flask solutions before and after attempting to detach *S. pasteurii* from the sand using a vortex-sonicate-vortex procedure. In the untreated condition, an abundance of viable *S. pasteurii* cells were detected before and after the vortex-

sonicate-vortex procedure for both planktonic cultures and for microbes attached to untreated sand (Figure 4). Solutions were

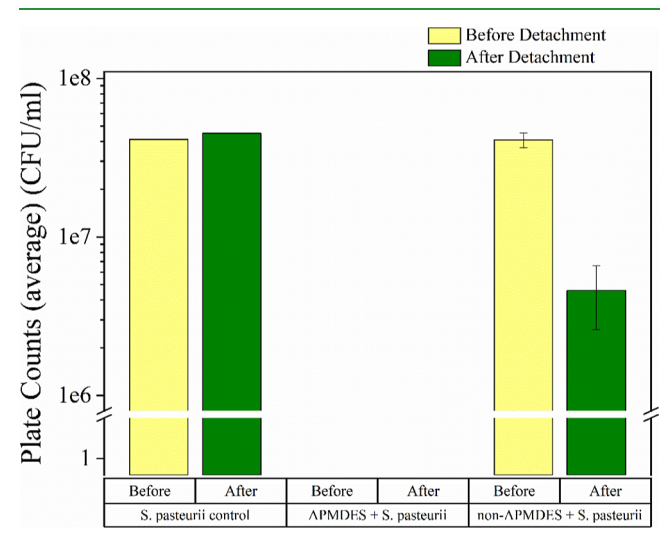


Figure 4. Plate counts of *S. pasteurii* from the supernatant before and after vortex-sonicate-vortex-induced detachment from sand, indicating that APMDES treatment of sand causes a loss of *S. pasteurii* viability.

replaced between the initial measurement and detached conditions, ensuring that viable microbes measured after the vortex-sonication-vortex steps had detached from sand. By contrast, no culturable cells were detected in APMDES-treated sand before or after the vortex-sonicate-vortex procedure. SEM images indicated that there was an abundance of microbes attached to sand in the APMDES-treated condition, both before and after the vortex-sonicate-vortex procedure (Figure 5). These results indicate that APMDES treatment results in strong attachment of *S. pasteurii* cells that resist detachment from sand and that *S. pasteurii* is not culturable under these conditions.

An additional imaging study was performed to visualize the impact of APMDES treatment on *S. pasteurii* at early time points. Confocal laser scanning microscopy (CLSM) was performed soon after *S. pasteurii* exposure to APMDES-treated sand (15 min) and 1 h after exposure (Figure 6). CLSM images showed green (Syto9-stained, nonmembrane-compromised cells) and red (propidium iodide-stained, membrane-compromised cells). Untreated sand showed very few cells at 15 min and sparse but mostly noncompromised (green) cells at 1 h (Figure 6A,B). By

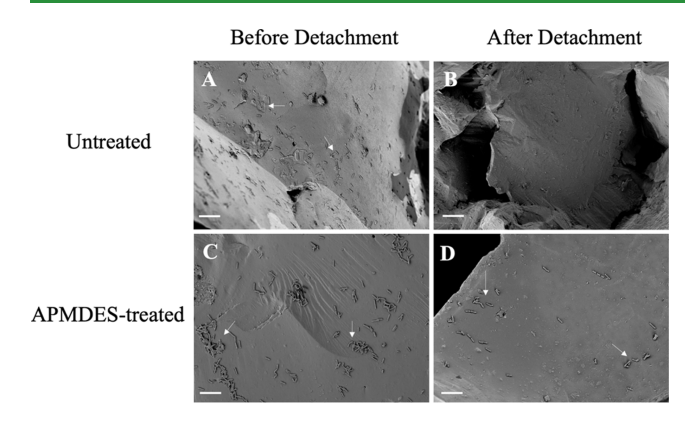


Figure 5. *S. pasteurii* cells were imaged on the surface of APMDES-treated and untreated sand before and after the detachment of microbes. (A,B) Untreated sand appears to have fewer microbes attached to its surface before and after detachment. (C,D) SEM images indicate higher numbers of microbes attached to APMDES-treated sand, both before and after the vortex-sonicate-vortex-induced attempt to detach microbes from sand surfaces. Scale bars are $10~\mu m$. White arrows indicate *S. pasteurii*.

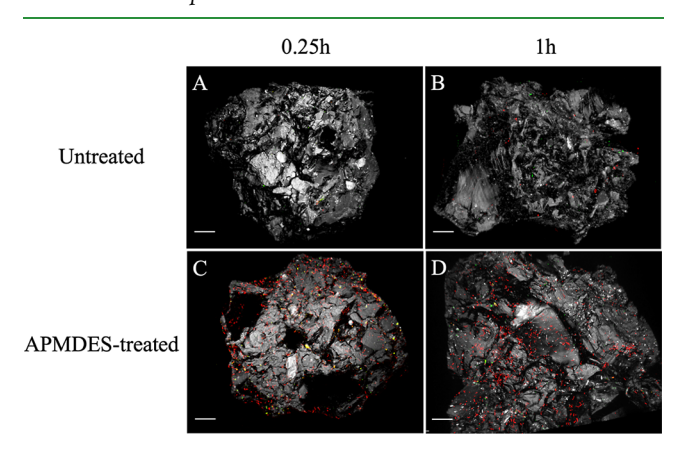


Figure 6. Initial attachment of *S. pasteurii* on APMDES-treated and untreated sand. (A,B) CLSM images demonstrate sparse but predominantly viable (green) microbes attached to untreated sand at 0.25 and 1 h. (C,D) Abundant microbial attachment is apparent on treated sand, with a mixture of viable (green) and membrane-compromised (red) microbes. Scale bars are 30 μ m.

contrast, APMDES-treated sand had abundant cells attached at both time points, with a small fraction of viable cells (green) but mostly membrane-compromised cells (red) (Figure 6C,D). Importantly, impaired membrane integrity visualized through this method can, but does not always, indicate impaired cell viability. 32,33

Together, these data indicate that APMDES is detrimental to *S. pasteurii*'s viability and growth. There are several potential reasons that may explain this effect. The increased electrostatic attraction between the cells and the treated surfaces could cause cell membrane damage. In support of this possibility, in other settings, positively charged surfaces have been reported to have antimicrobial effects due to strong electrostatic interactions disrupting cell membrane integrity. ¹⁶,18,31,34,35</sup>

Though APMDES treatment was detrimental to the growth and viability of *S. pasteurii* (Figures 3, 4, and 6), calcium carbonate precipitation still occurred reliably on the APMDES-treated sand. The decrease in urea concentrations over time in the bulk fluid during daily 8 h long biocementation periods indicated that urea hydrolysis was equivalent in both APMDES-

treated sand and untreated sand conditions (Figure 7), suggesting that the survival of cells exposed to APMDES was

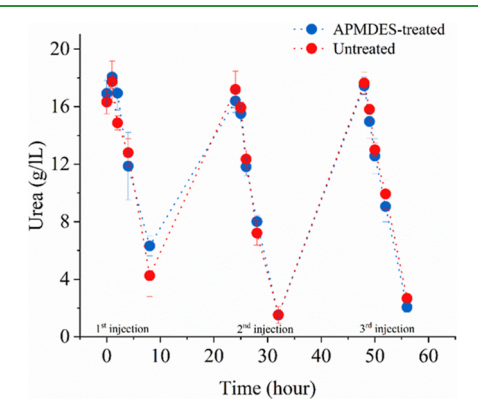


Figure 7. Urea concentrations (measured using a modified Jung assay) over time in the presence of APMDES-treated and untreated sand. Urea was added to an initial concentration of 20 g/L urea each day and was almost completely hydrolyzed during the 8 h time period.

not necessary for urea hydrolysis and biocementation. Importantly, cells and media were injected several times into both untreated and treated conditions, and the negative effects of APMDES on the viability of cells may decrease as the sand surface is increasingly covered with minerals.

The finding that urea hydrolysis does not depend on *S. pasteurii* viability under APMDES-treated conditions might contribute to the development of more efficient MICP processes, where the focus could be on urease enzyme functionality rather than maintaining high levels of cell viability. There are potential upsides for biocementation treatments that do not rely on preserving microbial viability. For example, the use of microbes in situations (e.g., outdoor usage) where their growth may disrupt the local soil microbiome may benefit from eliminating the viability of those cultures, whether through a treatment like APMDES or through another strategy (e.g., heat treatment, isolating the urease enzyme, etc.).

3.3. APMDES Treatment Decreases the Time Required for Strength Development via Biocementation. After determining that APMDES treatment increases the attachment of ureolytic microbes to sand, the next question was whether APMDES would impact the efficiency of strength gain through biocementation. For both APMDES-treated and untreated conditions, the minerals precipitated during biocementation were mostly calcite intermixed with minor fractions of vaterite, as confirmed by XRD (Figure 8). However, the appearance of cube and prism structures was markedly different with APMDES treatment. Structures manufactured using APMDES-treated sand had a much more precise edge definition than those made using untreated sand (Figure 9).

APMDES improved the compressive strength of cube specimens compared with that in the untreated condition (+49.7%, p = 0.007) (Figure 10, Table S1). After 3 injections, the mean compressive strength with APMDES treatment was almost double compared with that in untreated controls (2.31 vs 1.23 MPa). There was neither a significant effect of injections (p = 0.054) on compressive strength nor a significant interaction between injections and treatment (p = 0.147). It is noted that it is likely that this study was underpowered to detect the expected increase in strength with more injections and that including

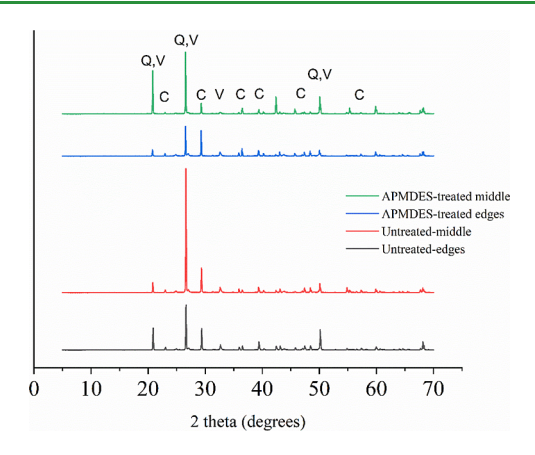


Figure 8. XRD spectra of 7 day biocemented cubes. Results reveal abundant calcite (C), with a minor vaterite (V) presence. Note that the largest vaterite peak overlaps with the quartz (Q), which is highly abundant for these samples.



Figure 9. Biocemented specimens after 3 injections. (A) $50 \text{ mm} \times 50$ mm cubes prepared using APMDES-treated sand. (B) 50 mm × 50 mm cubes prepared from untreated sand. (C) Prisms (25 mm × 25 mm × 90 mm) prepared from APMDES-treated sand (left) and untreated sand (right).

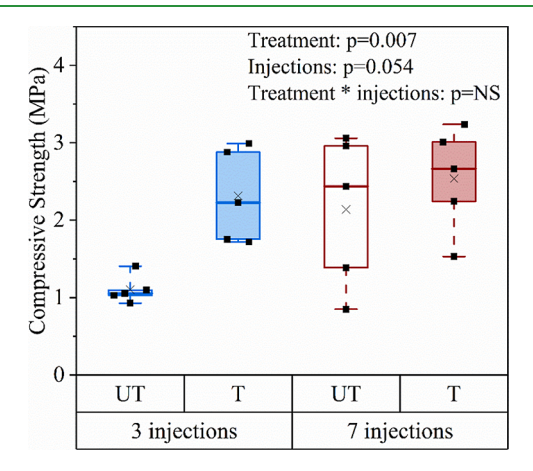


Figure 10. Compressive strength of APMDES-treated (T) and untreated (UT) cubes after 3 and 7 days of one injection daily. Boxplots show the median (line), mean (cross), interquartile range (box), minimum/maximum (whiskers), and individual data (dots).

additional specimens would be likely to increase the statistical significance.

The strength gain seen for APMDES-treated samples was rapid compared to that of the untreated controls as well as compared with data from other biocementation studies (Figure 11). For example, Bernardi and co-workers used S. pasteurii and

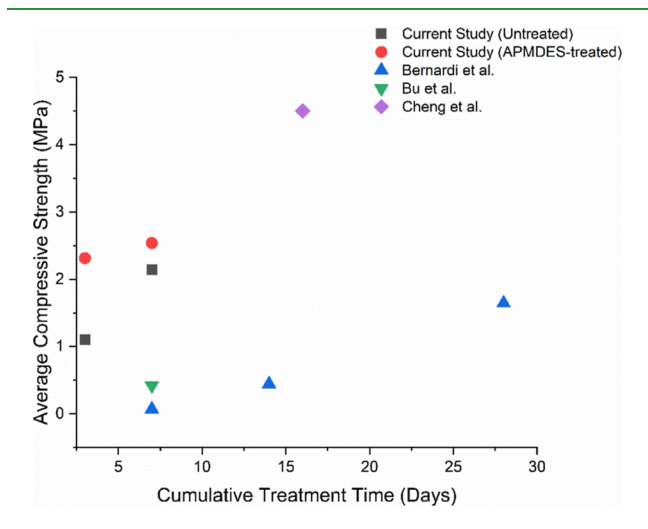


Figure 11. Relationships between cumulative MICP treatment time (days) and unconfined compressive strengths across findings from this study and other investigations. While all studies utilized silica sand, S. pasteurii, and similar constituents within biocementation media, there were differences in the sand size, media concentration, and biocementation procedures, which are detailed in Table S4.

urea-calcium medium to manufacture biobricks with dimensions of 91 mm \times 58 mm \times 200 mm. After 3 injections per day over 7 days (21 treatments), 14 days (42 treatments), or 28 days (84 treatments), they report achieving average compressive strengths of 0.07, 0.44, and 1.65 MPa, respectively.³⁶ Similarly, Lambert and Randall, 2019, developed brick-shaped specimens with dimensions of 222 mm \times 106 mm \times 73 mm using human urine as a urea source, which were biocemented for 8 days (6 injections per day, 48 treatments). This process produced specimens with an average compressive strength value of 2.7 MPa.³⁷ Bu et al. manufactured MICP-treated brick specimens with 177 mm \times 76 mm \times 38 mm dimensions, which had compressive strengths averaging 0.42 MPa after 1 treatment with 7 days of reaction. ³⁸ There are important differences across these studies in the type of microorganism, solution chemistry, size of the sand, and other characteristics that can influence the compressive strength. Regardless, APMDES treatment results in a very rapid strength development (average 2.1 MPa after 3 injections) compared to that of the most similarly shaped structures in literature. It is possible that additional injections beyond the end point of this study could further increase the strength of APMDES-treated materials, but this possibility requires additional investigation.

3.4. Strength Gain from APMDES Treatment Is Not Solely Explained by the Calcium-Containing Biomineral Gain. Because compressive strength has been shown to have a positive correlation with CaCO₃ accumulation, ^{13,14,16} the calcium-containing biomineral gain, which would be expected to largely represent CaCO3 accrual, was estimated by acid digestion (Figure 12). Biomineral gain depended on interactions between the number of injections and treatment (AMPDES vs no treatment) or region (i.e., edge or middle) (Figure 12A). Region and injection had an interactive effect (p = 0.003) on the weight percent of the calcium-containing biomineral gain. The

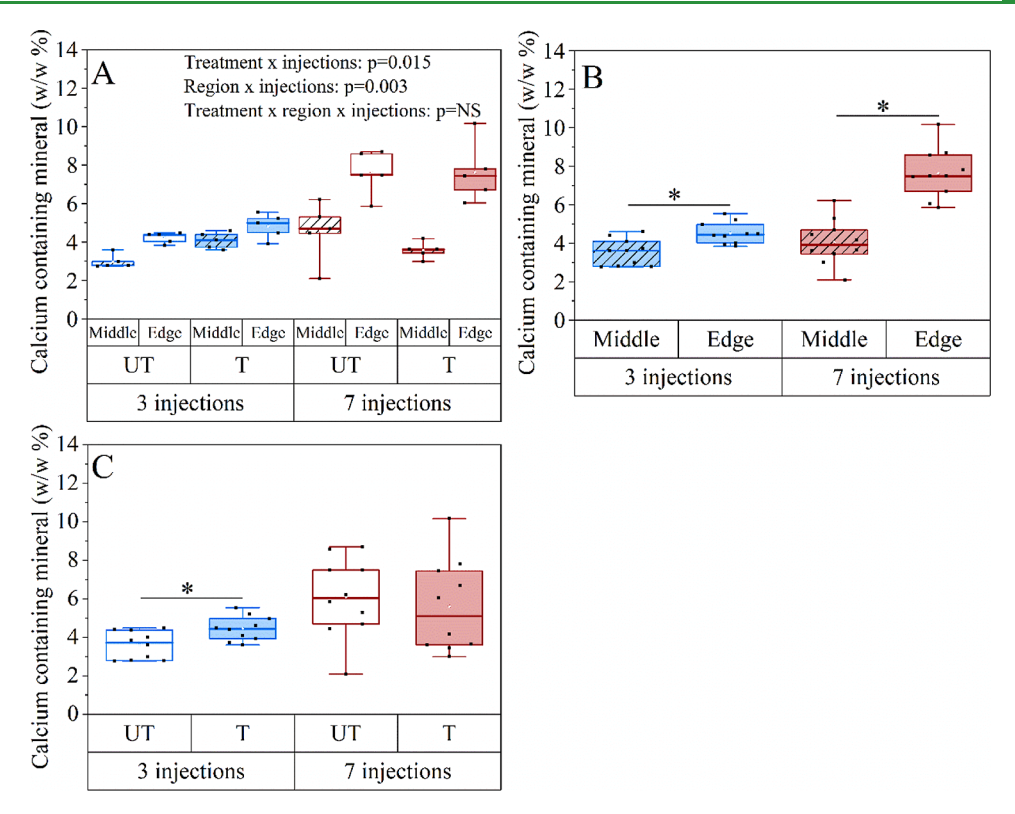


Figure 12. Treatment, region, and number of injections have interactive effects on the weight percent of calcium-containing mineral gain. (A) Biomineral gain estimated from acid digestion of edge and middle samples of sand cube specimens prepared with 3 or 7 injections. (B) Region-injection interaction effect on % calcium-containing minerals. (C) Treatment-injection effect on % calcium-containing minerals. Boxplots show the median (line), interquartile range (box), maximum and minimum (whiskers), and symbols representing all data points (squares). Significant simple effects from posthoc tests following significant interactions are indicated with asterisks.

outside (edges) of the cubes had more calcium-containing mineral compared to that in the center (middle) of the cubes manufactured with 3 injections (4.53% vs 3.54%, p = 0.006) and 7 injections (7.63% vs 4.06%, p < 0.001) (Figure 12B, Table S2). The effect of APMDES treatment was different between 3 day and 7 day injections (p = 0.015). APMDES-treated sand had a greater percentage of calcium-containing biomineral gain than untreated sand after 3 injections (4.46% vs 3.60%, p = 0.019), but calcium-containing biomineral gain was not different between APMDES-treated sand and untreated sand after 7 injections (p = 0.280) (Figure 12C, Table S3).

Since APMDES increased strength at 3 and 7 injections but the calcium-containing biomineral gain was only higher at 3 injections, ANCOVA was used to test the relationship between strength and calcium gain. After accounting for the linear, positive relationship with the calcium content through ANCOVA, there was still a significant effect of APMDES treatment on compressive strength (p=0.029). These data demonstrate that strength gain with APMDES treatment is likely not solely attributed to the greater accumulation of biominerals (Figure 13).

Because APMDES treatment appears to alter the relationship between biomineral accumulation and strength gain, the geometry of biomineral bridges was investigated from embedded and polished sections of biocemented cubes. There were several statistically significant microstructural differences between the APMDES-treated and untreated conditions, such as increased sphericity and decreased size for calcium carbonate bridges in the APMDES-treated structure (Table 1). This result could indicate a difference in how biomineral bridges nucleate

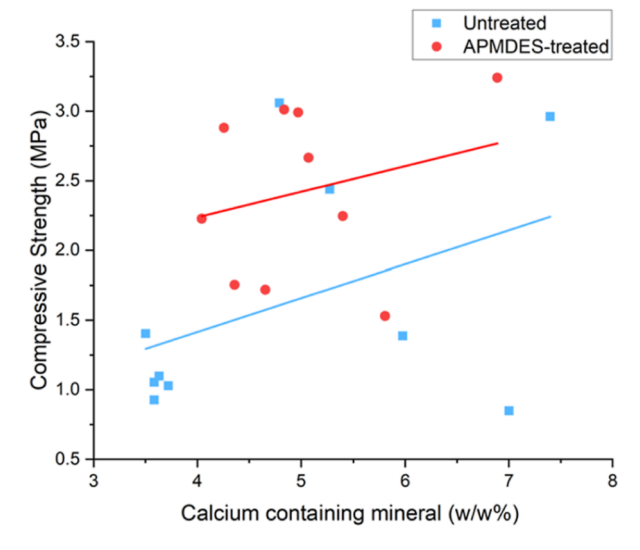


Figure 13. Mean calcium-containing biomineral gain versus compressive strength of specimens prepared with untreated ($r^2 = 0.18$) or APMDES-treated ($r^2 = 0.06$) sand combining 3 and 7 injection data. A regression line is shown for each condition.

and grow with the APMDES treatment. Other measures were not significantly different between the treated and untreated groups (Table 1).

3.5. Implications for Sustainability. Biocementation has garnered considerable attention as a lower-temperature process for building load-bearing materials or improving soils, but sustainability decreases as the number of injections of bacteria

Table 1. Biomineral Bridge Geometric Characteristics from SEM-EDX Maps of Calcium (Biomineral Bridges) and Silicon (Sand Grains) (Figure S2)^a

measure	untreated	APMDES-treated	<i>p</i> -value
mean total sand area	$22.99 \pm 1.39 \text{ mm}^2$	$24.60 \pm 0.88 \text{ mm}^2$	0.069
mean number of sand grains	39.33 ± 2.52	38.56 ± 3.47	0.227
mean total CaCO ₃ area	$2.65 \pm 0.91 \text{ mm}^2$	$1.89 \pm 0.67 \text{ mm}^2$	0.189
mean CaCO ₃ area/sand area	0.120 ± 0.0490	0.0788 ± 0.0302	0.141
mean number of biomineral bridges	84.22 ± 8.88	86.89 ± 14.26	0.295
mean biomineral bridge number/sand grain number	2.189 ± 0.178	2.256 ± 0.345	0.837
mean biomineral bridge area	$0.031 \pm 0.012 \text{ mm}^2$	$0.021 \pm 0.006 \text{ mm}^2$	0.045
mean biomineral bridge major axis	$0.29 \pm 0.048 \text{ mm}$	$0.24 \pm 0.032 \text{ mm}$	0.133
mean biomineral bridge minor axis	$0.14 \pm 0.027 \text{ mm}$	$0.11 \pm 0.015 \text{ mm}$	0.073
mean biomineral bridge circularity (minor/major axes)	0.49 ± 0.050	0.55 ± 0.029	0.033

^aMeans were calculated from three specimens where each represents the mean of three randomly selected regions of interest. Data are presented as the mean \pm standard deviation.

and nutrients increases.³⁹ APMDES treatment may increase the sustainability of bacterial biocementation by decreasing the number of injections required to achieve a target compressive strength. Further, biocementation using ureolytic microbes produces ammonia, which is not desirable in some locations and situations. APMDES treatment has the potential to improve the sustainability of biocementation treatment by decreasing the number of inputs (i.e., injections) and waste outputs. It is important to note that functionalizing the sand surface with silane coupling agents increases the energy requirements of creating the biocemented structure as the sand undergoes drying and ozone treatment steps, which require energy inputs. This treatment process also requires the production and disposal of chemicals, including ethanol, acetone, and APMDES. A full comparative life cycle analysis of APMDES treatment versus conventional biocementation was outside of the scope of the present investigation but would be valuable for comparing the two manufacturing methods.

3.6. Limitations. This study has several important limitations. While the APMDES treatment was reported to increase strength development for similar biomineral content, the specific mechanisms contributing to this strength development require further investigation. Additionally, while microscopy images provided qualitative evidence of increased microbial density on APMDES-treated sand surfaces, it is not known whether the APMDES treatment and subsequent bacterial distribution were homogeneous within all areas of the sand matrix. In this study, we did not investigate whether strength gain would continue past 7 injections, but this would merit future investigation. Furthermore, the dynamics of how microbial attachment, nucleation, and growth are impacted for the first treatment versus subsequent treatments are not answered here. Additional research is needed to gain a better understanding of how these treatments affect biomineral nucleation and growth and the resulting strength development. Furthermore, prior experimentation with -NH₃⁺ moieties shows that these ions are toxic to some bacteria but not to others.³⁴ Additional careful study is required to identify combinations of bacteria and surface charges that achieve goals of either viability or nonviability depending on the intended applications. Another limitation is that only silica sand was investigated in this study. The effectiveness of APMDES treatment to improve the efficiency of biocementation may vary with soil type and should be investigated in future work. More broadly, further work is required to explore the feasibility of utilizing APMDES treatment for larger-scale applications,

including the potential simplification of treatment steps and also the study of cellular attachment and viability under these conditions.

4. CONCLUSIONS

This study demonstrates that the use of amino silane coupling agents, such as APMDES, can be an effective method for improving the efficiency in strength development during bacterial biocementation. The key findings of this research were that APMDES treatment altered the surface properties of sand, which resulted in increased attraction for ureolytic bacteria and improved strength development over a shorter period of time. APMDES achieved this strength gain without increasing the quantity of calcium-containing biominerals within the structure, indicating an alteration of other characteristics contributing to strength. Overall, these results suggest that aggregate pretreatment methods such as amino silane coupling agents may offer promising solutions for improving efficiency and effectiveness outcomes related to microbial biomineralization.

ASSOCIATED CONTENT

Supporting Information

The Supporting Information is available free of charge at https://pubs.acs.org/doi/10.1021/acsami.3c13971.

3D print model of molds, SEM—EDX map of biomineral bridges, effects of APMDES treatment on compressive strength, effects of number of injections and region on biomineral accumulation, effects of number of injections and treatment on biomineral accumulation, and comparison of experimental designs in highlighted studies (PDF)

AUTHOR INFORMATION

Corresponding Author

Chelsea Heveran — Mechanical and Industrial Engineering
Department, Montana State University, Bozeman, Montana
S9717, United States; Center for Biofilm Engineering,
Montana State University, Bozeman, Montana S9717, United
States; orcid.org/0000-0002-1406-7439;
Email: chelsea.heveran@montana.edu

Authors

Gizem Elif Ugur — Mechanical and Industrial Engineering Department, Montana State University, Bozeman, Montana 59717, United States

- Kylee Rux Civil and Environmental Engineering Department, Montana State University, Bozeman, Montana 59717, United States
- John Connor Boone Mechanical and Industrial Engineering Department, Montana State University, Bozeman, Montana 59717, United States
- Rachel Seaman Center for Biofilm Engineering, Montana State University, Bozeman, Montana 59717, United States
- Recep Avci Department of Physics, Montana State University, Bozeman, Montana 59717, United States
- Robin Gerlach Center for Biofilm Engineering and Chemical & Biological Engineering Department, Montana State University, Bozeman, Montana 59717, United States; orcid.org/0000-0002-7669-3072
- Adrienne Phillips Civil and Environmental Engineering Department and Center for Biofilm Engineering, Montana State University, Bozeman, Montana 59717, United States

Complete contact information is available at: https://pubs.acs.org/10.1021/acsami.3c13971

Author Contributions

G.E.U.: conceptualization, methodology, formal analysis, investigation, data curation, writing—original draft, visualization, and writing—review and editing. K.R.: formal analysis, investigation, visualization, and writing—review and editing. J.C.B.: software, formal analysis, and writing—review and editing. R.S.: investigation, visualization, and writing—review and editing. R.A.: resources and writing—review and editing. R.G.: writing—review and editing, supervision, and funding acquisition. A.P.: conceptualization, resources, writing—review and editing, supervision, and funding acquisition. C.M.H.: conceptualization, formal analysis, resources, data curation, writing—original draft, writing—review and editing, supervision, project administration, and funding acquisition.

Funding

The authors gratefully acknowledge support from the National Science Foundation (C.H., A.P., R.G.: 2036867; C.H., R.G., R.A.: 2328351; R.A.: 2025391). Any opinions, findings, conclusions, or recommendations expressed in this material are those of the authors and do not necessarily reflect the views of the National Science Foundation.

Notes

The authors declare the following competing financial interest(s): R.A. is the inventor of patent US 20160320277 A1, which includes biotrapping technology. This patent is not currently licensed to any entities.

ACKNOWLEDGMENTS

The authors appreciate assistance from the staff of the Montana State University Center for Biofilm Engineering (Dr. Heidi Smith) and the Image and Chemical Analysis Laboratory (Dr. Sara Zacher). Imaging was made possible by the Center for Biofilm Imaging Facility at Montana State University, which is supported by funding from the National Science Foundation MRI Program (2018562), the M. J. Murdock Charitable Trust (202016116), and the US Department of Defense (77369LSRIP). Additionally, the authors appreciate Kenna Brown's assistance in designing 3D-printed molds and Allyson Bomber's assistance with acid digestion.

ABBREVIATIONS

APMDES, 3-aminopropyl-methyl-diethoxysilane; MICP, microbially induced calcium carbonate precipitation; BHI, brain heart infusion; CMM+, calcium-containing medium; CMM-, calcium-free medium; CLSM, confocal laser scanning microscopy; PMT, photomultiplier tube; SEM, scanning electron microscopy

REFERENCES

- (1) Izumi, Y.; Iizuka, A.; Ho, H. J. Calculation of greenhouse gas emissions for a carbon recycling system using mineral carbon capture and utilization technology in the cement industry. *J. Cleaner Prod.* **2021**, 312, 127618.
- (2) Teh, S. H.; Wiedmann, T.; Castel, A.; de Burgh, J. Hybrid life cycle assessment of greenhouse gas emissions from cement, concrete and geopolymer concrete in Australia. *J. Cleaner Prod.* **2017**, *152*, 312–320.
- (3) Achal, V.; Mukherjee, A. A review of microbial precipitation for sustainable construction. *Constr. Build. Mater.* **2015**, 93, 1224–1235.
- (4) Zhang, W.; Zheng, Q.; Ashour, A.; Han, B. Self-healing cement concrete composites for resilient infrastructures: A review. *Composites, Part B* **2020**, *189*, 107892.
- (5) Phillips, A. J.; Cunningham, A. B.; Gerlach, R.; Hiebert, R.; Hwang, C.; Lomans, B.; Westrich, J.; Mantilla, C.; Kirksey, J.; Esposito, R.; Spangler, L. Fracture Sealing with Microbially-Induced Calcium Carbonate Precipitation: A Field Study. *Environ. Sci. Technol.* **2016**, *50* (7), 4111–4117.
- (6) Mujah, D.; Shahin, M. A.; Cheng, L. State-of-the-Art Review of Biocementation by Microbially Induced Calcite Precipitation (MICP) for Soil Stabilization. *Geomicrobiol. J.* **2017**, *34* (6), 524–537.
- (7) De Muynck, W.; De Belie, N.; Verstraete, W. Microbial carbonate precipitation in construction materials: A review. *Ecol. Eng.* **2010**, *36* (2), 118–136.
- (8) Phillips, A. J.; Gerlach, R.; Lauchnor, E.; Mitchell, A. C.; Cunningham, A. B.; Spangler, L. Engineered applications of ureolytic biomineralization: a review. *Biofouling* **2013**, 29 (6), 715–733.
- (9) Victoria, S. W. Microbial CaCO3 Precipitation for the Production of Biocement, Ph.D. Thesis, Murdoch University, 2004
- (10) Cheng, L.; Cord-Ruwisch, R.; Shahin, M. A. Cementation of sand soil by microbially induced calcite precipitation at various degrees of saturation. *Can. Geotech. J.* **2013**, *50* (1), 81–90.
- (11) Xiao, Y.; He, X.; Zaman, M.; Ma, G.; Zhao, C. Review of Strength Improvements of Biocemented Soils. *Int. J. Geomech* **2022**, 22 (11), 03122001.
- (12) Whiffin, V. S.; van Paassen, L. A.; Harkes, M. P. Microbial Carbonate Precipitation as a Soil Improvement Technique. *Geomicrobiol. J.* **2007**, 24 (5), 417–423.
- (13) Achal, V.; Mukherjee, A.; Kumari, D.; Zhang, Q. Biomineralization for sustainable construction A review of processes and applications. *Earth-Sci. Rev.* **2015**, *148*, 1–17.
- (14) Rajasekar, A.; Moy, C. K. S.; Wilkinson, S. MICP and Advances towards Eco-Friendly and Economical Applications. *IOP Conf. Ser. Earth Environ. Sci.* **2017**, *78*, 012016.
- (15) Harkes, M. P.; van Paassen, L. A.; Booster, J. L.; Whiffin, V. S.; van Loosdrecht, M. C. M. Fixation and distribution of bacterial activity in sand to induce carbonate precipitation for ground reinforcement. *Ecol. Eng.* **2010**, *36* (2), 112–117.
- (16) Avci, R. BiyoTrap. U.S Patent 20,160,320,277 A1. 2019.
- (17) Rzhepishevska, O.; Hakobyan, S.; Ruhal, R.; Gautrot, J.; Barbero, D.; Ramstedt, M. The surface charge of anti-bacterial coatings alters motility and biofilm architecture. *Biomater. Sci.* **2013**, *1* (6), 589.
- (18) Metwally, S.; Stachewicz, U. Surface potential and charges impact on cell responses on biomaterials interfaces for medical applications. *Mater. Sci. Eng. Carbon* **2019**, *104*, 109883.
- (19) Oh, J. K.; Yegin, Y.; Yang, F.; Zhang, M.; Li, J.; Huang, S.; Verkhoturov, S.; Schweikert, E.; Perez-Lewis, K.; Scholar, E.; Taylor, T. M.; Castillo, A.; Cisneros-Zevallos, L.; Min, Y.; Akbulut, M. The influence of surface chemistry on the kinetics and thermodynamics of bacterial adhesion. *Sci. Rep.* **2018**, *8* (1), 17247.

- (20) Rimola, A.; Costa, D.; Sodupe, M.; Lambert, J. F.; Ugliengo, P. Silica Surface Features and Their Role in the Adsorption of Biomolecules: Computational Modeling and Experiments. *Chem. Rev.* **2013**, *113* (6), 4216–4313.
- (21) Martin, J. Biocorrosion of 1018 Steel in Sulphide Richmarine Environments; a Correlation between Strain and Corrosion Using Electron Backscatter Diffraction, MS thesis, Montana State University, 2014.
- (22) Aydin, Ş. C. Rapid Detection and Identification of Bacterial Pathogens in Drinking Water Sources Using DNA-Based Methods and Immunoimmobilization Technology; Bogazici University, 2007.
- (23) Suo, Z.; Avci, R.; Yang, X.; Pascual, D. W. Efficient Immobilization and Patterning of Live Bacterial Cells. *Langmuir* **2008**, 24 (8), 4161–4167.
- (24) Suo, Z.; Yang, X.; Avci, R.; Deliorman, M.; Rugheimer, P.; Pascual, D.; Idzerda, Y. Antibody Selection for Immobilizing Living Bacteria. *Anal. Chem.* **2009**, *81* (18), 7571–7578.
- (25) Yadav, A. R.; Sriram, R.; Carter, J. A.; Miller, B. L. Comparative study of solution—phase and vapor—phase deposition of aminosilanes on silicon dioxide surfaces. *Mater. Sci. Eng. Carbon* **2014**, *35*, 283—290.
- (26) Jung, D.; Biggs, H.; Erikson, J.; Ledyard, P. U. New Colorimetric Reaction for End-Point, Continuous-Flow, and Kinetic Measurement of Urea. *Clin. Chem.* **1975**, *21* (8), 1136–1140.
- (27) Herigstad, B.; Hamilton, M.; Heersink, J. How to optimize the drop plate method for enumerating bacteria. *J. Microbiol. Methods* **2001**, 44 (2), 121–129.
- (28) Otsu, N. A. Threshold Selection Method from Gray-Level Histograms. *IEEE Trans. Syst. Man Cybern. Syst.* 1979, 9, 62–66.
- (29) Deliorman, M. The Immunoimmobilization of Living Bacteria on Solid Surfaces and its Applications; Montana State University, 2012.
- (30) Ma, L.; Pang, A. P.; Luo, Y.; Lu, X.; Lin, F. Beneficial factors for biomineralization by ureolytic bacterium Sporosarcina pasteurii. *Microb. Cell Factories* **2020**, *19* (1), 12.
- (31) Jennings, M. C.; Minbiole, K. P. C.; Wuest, W. M. Quaternary Ammonium Compounds: An Antimicrobial Mainstay and Platform for Innovation to Address Bacterial Resistance. *ACS Infect. Dis.* **2015**, *1* (7), 288–303.
- (32) Berney, M.; Hammes, F.; Bosshard, F.; Weilenmann, H. U.; Egli, T. Assessment and Interpretation of Bacterial Viability by Using the LIVE/DEAD BacLight Kit in Combination with Flow Cytometry. *Appl. Environ. Microbiol.* **2007**, 73 (10), 3283–3290.
- (33) Stiefel, P.; Schmidt-Emrich, S.; Maniura-Weber, K.; Ren, Q. Critical aspects of using bacterial cell viability assays with the fluorophores SYTO9 and propidium iodide. *BMC Microbiol.* **2015**, 15 (1), 36.
- (34) Murata, H.; Koepsel, R. R.; Matyjaszewski, K.; Russell, A. J. Permanent, non-leaching antibacterial surfaces—2: How high density cationic surfaces kill bacterial cells. *Biomaterials* **2007**, *28* (32), 4870—4870
- (35) Nihei, T. Antimicrobial Activity of a Novel Silane Coupling Agent Consisting of a Quaternary Ammonium Salt Using a Polymicrobial Biofilm Model. *J. dent health oral disord. ther.* **2017**, 7 (4), 301.
- (36) Bernardi, D.; DeJong, J. T.; Montoya, B. M.; Martinez, B. C. Biobricks: Biologically cemented sandstone bricks. *Constr. Build. Mater.* **2014**, 55, 462–469.
- (37) Lambert, S. E.; Randall, D. G. Manufacturing bio-bricks using microbial induced calcium carbonate precipitation and human urine. *Water Res.* **2019**, *160*, 158–166.
- (38) Bu, C.; Wen, K.; Liu, S.; Ogbonnaya, U.; Li, L. Development of bio-cemented constructional materials through microbial induced calcite precipitation. *Mater. Struct.* **2018**, *51* (1), 30.
- (39) Porter, H.; Mukherjee, A.; Tuladhar, R.; Dhami, N. K. Life Cycle Assessment of Biocement: An Emerging Sustainable Solution? *Sustainability* **2021**, *13* (24), 13878.